Surgical Endoscopy
https://doi.org/10.1007/s00464-026-13307-1

Thoracoscopic surgery for congenital pulmonary malformations in infants: a preliminary comparative evaluation of virtual reality-guided preoperative planning versus standard imaging

Ugo Maria Pierucci[1,2] · Irene Paraboschi[1,2] · Sara Costanzo[1] · Carlotta Ardenghi[1] · Michela Marinaro[1] · Alessia Musitelli[1] · Michele Ceresola[1] · Eleonora Durante[1] · Sara Baroni[1] · Francesco Rizzetto[3,4] · Salvatore Zirpoli[5] · Cristina Gallotta[6] · Maurizio Vertemati[2,6] · Valeria Calcaterra[7,8] · Gianvincenzo Zuccotti[2,7] · Gloria Pelizzo[1,2]

Received: 11 May 2026 / Accepted: 12 August 2026
© The Author(s), under exclusive licence to Springer Science+Business Media, LLC, part of Springer Nature 2026

Abstract

Background Thoracoscopic resection of congenital pulmonary malformations remains technically demanding because of limited working space, variable broncho-vascular anatomy and the need to preserve healthy lung parenchyma. An integrated workflow combining patient-specific three-dimensional (3D) segmentation with immersive virtual reality (VR) navigation may enhance preoperative planning, but clinical data remain limited.

Methods We performed a retrospective historical cohort study of children undergoing thoracoscopic resection between 2013 and 2024. Patients were grouped according to planning strategy: standard imaging (SI) alone or an additional integrated workflow combining patient-specific 3D segmentation with immersive VR navigation (VR). Perioperative outcomes were compared, with focused analyses of lesion and procedure heterogeneity and chronological effects.

Results Fifty infants were analyzed (39 SI, 11 VR). Median operative time was 183 versus 248 min ($p = 0.42$). Conversion occurred in 10/39 SI cases and no VR cases ($p = 0.045$); intraoperative complications occurred in 5/39 and 0/11 ($p = 0.20$), and postoperative complications in 6/39 and 0/11 ($p = 0.16$). Median NICU/PICU stay was 2 versus 1 day ($p = 0.045$), and hospital stay 8 versus 5 days ($p < 0.001$). Three SI patients required redo surgery and no VR patients did. Findings showed substantial case-mix heterogeneity, but their favorable direction was maintained in focused analyses. VR cases occurred later in the institutional experience.

Conclusions The integrated VR-guided workflow was feasible and associated with favorable perioperative signals. Although the historical design precludes causal attribution, the consistency of these preliminary findings supports prospective evaluation of VR as a patient-specific planning adjunct.

Keywords Congenital pulmonary malformations · Thoracoscopic surgery · Virtual reality · 3D imaging · Preoperative planning · Pediatric minimally invasive surgery

✉ Ugo Maria Pierucci
ugomariapierucci@icloud.com

✉ Gloria Pelizzo
gloria.pelizzo@unimi.it

[1] Department of Pediatric Surgery, "V. Buzzi" Children's Hospital, 20154 Milano, Italy

[2] Department of Biomedical and Clinical Science, University of Milano, 20157 Milano, Italy

[3] Department of Radiology, ASST Grande Ospedale Metropolitano Niguarda, 20162 Milano, Italy

[4] Postgraduate School of Diagnostic and Interventional Radiology, University of Milano, 20122 Milano, Italy

[5] Department of Pediatric Radiology, "V. Buzzi" Children's Hospital, 20154 Milan, Italy

[6] CIMaINa (Interdisciplinary Centre for Nanostructured Materials and Interfaces), University of Milano, 20133 Milano, Italy

[7] Pediatric Department, "V. Buzzi" Children's Hospital, 20154 Milano, Italy

[8] Pediatrics and Adolescentology Unit, Department of Internal Medicine, University of Pavia, 27100 Pavia, Italy

Published online: 25 August 2026

Abbreviations

3D	Three-dimensional
CNS	Central nervous system
CPAM	Congenital pulmonary airway malformation
CPMs	Congenital pulmonary malformations
CT	Computed tomography
CVS	Cardiovascular system
DICOM	Digital imaging and communications in medicine
ESP	Erector spinae plane (block)
GI	Gastrointestinal
HMD	Head-mounted display
IQR	Interquartile range
LOS	Length of stay
MRI	Magnetic resonance imaging
NICU	Neonatal intensive care unit
PICU	Pediatric intensive care unit
SD	Standard deviation
SI	Standard imaging
VR	Virtual reality

Congenital pulmonary malformations (CPM), including congenital pulmonary airway malformations (CPAM), intralobar and extralobar sequestration, bronchogenic cysts, congenital lobar overinflation, and bronchial atresia are increasingly identified through routine prenatal imaging and are now often managed electively during infancy [1–3]. Although thoracoscopic resection has become the preferred approach in many centers, it remains technically challenging in small infants because of limited intrathoracic operative space, complex segmental anatomy, and the need to preserve healthy lung tissue [4, 5]. Even in experienced hands, these challenges can influence operative time, conversion rates, and postoperative recovery [6, 7]. In recent years, virtual reality (VR) has emerged as a powerful tool for preoperative planning, enabling an accurate patient-specific three-dimensional (3D) representation of complex anatomy. In our workflow, segmentation and immersive VR navigation are not separate interventions: the source CT or MRI dataset is segmented to generate the patient-specific model that is subsequently explored within a head-mounted immersive environment. VR allows surgeons to visualize and interact with malformations, vessels, and bronchi in a life-like spatial context. Moreover, virtual preoperative navigation of the malformation and hilar structures allows the surgical team to rehearse the stages of the operation by evaluating risks, possible complications and ways to avoid them. Although the anatomical information derives from the same source imaging, immersive VR adds stereoscopic depth, interactive navigation, adjustable transparency, operative-perspective orientation and shared multidisciplinary review. Our group previously introduced a VR workflow based on head-mounted display (HMD) for pediatric surgical planning, demonstrating its feasibility and value in visualizing complex CPM [8]. In that pilot experience, immersive 3D visualization improved preoperative orientation, aided in the identification of anomalous vascular connections, and supported port mapping tailored to the thoracoscopic position. Subsequently, in a larger multicenter pediatric series, VR planning influenced surgical strategy in a significant proportion of cases, improving spatial understanding and confidence across several subspecialties, with CPM representing one of the most frequent indications [9]. Despite these encouraging observations, quantitative evidence on clinical outcomes in infants undergoing thoracoscopic resection of CPM remains limited. To address this gap, we evaluated this integrated VR-based preoperative planning workflow, comparing perioperative outcomes with standard imaging while explicitly exploring lesion heterogeneity, resection type and potential learning curve or era effects.

Materials and methods

This retrospective historical cohort study was conducted at the Department of Pediatric Surgery, "Vittore Buzzi" Children's Hospital, University of Milano, Italy, which serves as a tertiary referral center for pediatric minimally invasive thoracic surgery. The study is reported in accordance with the STROBE recommendations for observational studies. The study period extended from January 2013 to December 2024. All infants who underwent thoracoscopic surgery for CPM during the study period were eligible for inclusion. Demographic, clinical, and perinatal data were retrospectively collected from institutional medical records together with preoperative imaging, intraoperative findings, and postoperative outcomes. Each patient had undergone comprehensive preoperative imaging, including chest X-ray and computed tomography (CT) and/or magnetic resonance imaging (MRI), to define the extent and morphology of the lesion. According to the preoperative planning approach, patients were categorized into two groups. The first group underwent conventional planning based solely on standard radiologic imaging (SI), which consisted of axial, coronal, sagittal and multiplanar CT or MRI reconstructions reviewed on a workstation; these patients did not have access to a patient-specific segmented 3D model. The second group underwent the integrated VR workflow: source imaging was segmented to generate a patient-specific 3D model, which was subsequently explored within a head-mounted immersive environment. Three-dimensional segmentation and immersive navigation were therefore consecutive and inseparable components of a single planning workflow. VR planning was introduced during the later phase of

the institutional experience; therefore, the groups were non-concurrent, allocation was not randomized and was influenced by workflow availability, imaging suitability for segmentation and perceived anatomical complexity.

Three-dimensional (3D) reconstruction

CT datasets were acquired with 0.6-mm-thick slices during arterial and venous phases to optimize the visualization of pulmonary and systemic vascular structures. DICOM files were imported into 3D Slicer v.4.11 (https://www.slicer.org) [10], an open-source platform for medical image segmentation and 3D rendering. A mixed segmentation workflow was applied, combining deep learning-based automatic models [11] with threshold-based and region-growing semi-automatic algorithms, along with manual corrections, to precisely delineate the contours of lung parenchyma, the malformation, and the tracheobronchial and vascular structures. The resulting segmentations were optimized for subsequent post-processing and converted into 3D surface models that could be freely rotated, zoomed and displayed with adjustable transparency, allowing detailed assessment of internal vascularization and spatial relationships. Each segmentation was independently reviewed and validated by a pediatric radiologist to ensure consistency with the original imaging data. This segmentation constituted the technical basis of the immersive VR environment and was not evaluated as a separate desktop-planning intervention. Figure 1 illustrates the workflow used for patient-specific reconstruction, from raw CT imaging to semi-automatic segmentation and final 3D rendering integrated into the immersive VR environment for surgical planning.

Virtual reality (VR) workflow

Validated 3D models were transferred to a HMD using an in-house plugin developed for 3D Slicer. The system employed the Meta Quest 3 (Meta Platforms, Inc., Menlo Park, CA, USA), an all-in-one HMD. A tailored application allowed the surgical team to explore the reconstruction interactively in an immersive virtual reality environment, providing a comprehensive view of the anatomical structures of interest [12]. During preoperative planning sessions, surgeons could navigate around and within the model and manipulate it by rotating, zooming or adjusting transparency to analyze the anatomical relationships between the malformation, bronchi, vessels and parenchyma and to anticipate resection planes. The active immersive view was simultaneously mirrored on an external monitor, enabling surgeons, radiologists, anesthesiologists and trainees to participate in real-time discussion and planning; desktop visualization was not evaluated as a separate intervention. All reconstructions were oriented according to the patient's intraoperative lateral decubitus position to replicate the thoracoscopic view and facilitate preoperative port mapping [8, 9].

Preoperative evaluation and intraoperative correlation

The patient-specific models were reviewed in conjunction with the source CT or MRI images to evaluate their fidelity and clinical usefulness. During surgery, intraoperative findings were systematically compared with the preoperative 3D models to verify correspondence between the virtual model and actual anatomy, particularly regarding vascular and bronchial branching patterns [8, 9].

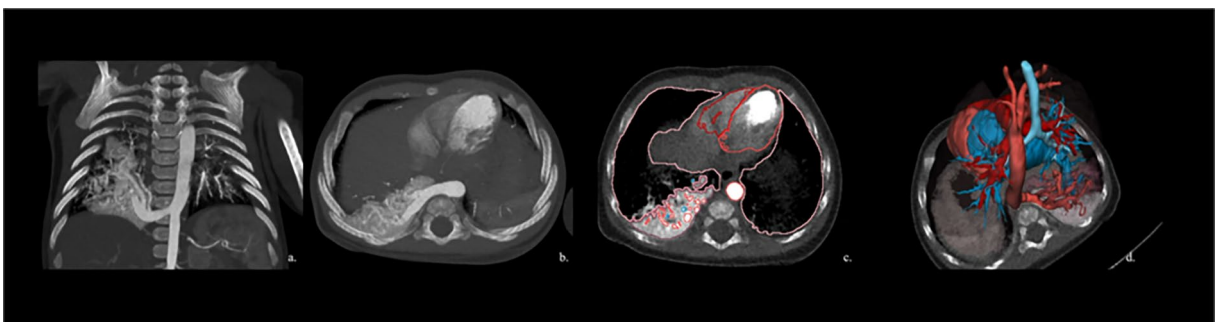


Fig. 1 Example of the virtual reality (VR) workflow for patient-specific three-dimensional (3D) reconstruction of a congenital pulmonary malformation. **a** Coronal contrast-enhanced CT reconstruction demonstrating a left lower-lobe congenital pulmonary malformation with anomalous systemic arterial supply. **b** Axial contrast-enhanced CT image highlighting the lesion and its relationship with surrounding mediastinal and diaphragmatic structures. **c** Semi-automatic segmentation performed in 3D Slicer v.4.11, combining threshold-ing, region-growing, and manual refinement to delineate lung parenchyma, malformation, and vascular structures (outlined in red). **d** Final 3D surface rendering illustrating the spatial relationships between pulmonary arteries (red), pulmonary veins (blue), systemic vessels, and the lesion, subsequently integrated into the immersive virtual reality environment for preoperative planning, port mapping, and multidisciplinary team discussion

Surgical technique

All operations were performed under general anesthesia with single-lung ventilation achieved using an Arndt endobronchial blocker (Cook®, USA). Patients were positioned in lateral decubitus, and a continuous erector spinae plane (ESP) block was maintained for perioperative analgesia. The thoracoscopic approach included two camera ports along the mid-axillary line, allowing flexible alternation between apical and basal visualization, and two working ports placed medially and laterally for optimal instrument ergonomics. Depending on the lesion's location and extension, either lobectomy or lung-sparing resection was performed. A mirrored view of the patient-specific immersive model was available in the operating room for anatomical reference during the procedure; this was not a separately evaluated desktop intervention. Representative correlations between the immersive VR reconstructions and the thoracoscopic view for different types of CPM are shown in Fig. 2. All procedures included in this analysis were performed or directly supervised by senior pediatric surgeons with established experience in minimally invasive thoracic surgery and thoracoscopic management of CPM.

Statistical analysis

Continuous variables were expressed as mean ± standard deviation or median (interquartile range, IQR), according to data distribution. Categorical variables were expressed as *n*/*N* (%). Between-group comparisons were performed using the Mann–Whitney *U* test or Student's *t* test for continuous variables, and Fisher's exact test for categorical variables, as appropriate. Because of the exploratory nature of the study, the small size of the VR cohort and the chronological separation between groups, analyses were interpreted primarily descriptively, avoiding causal inference based on *p* values

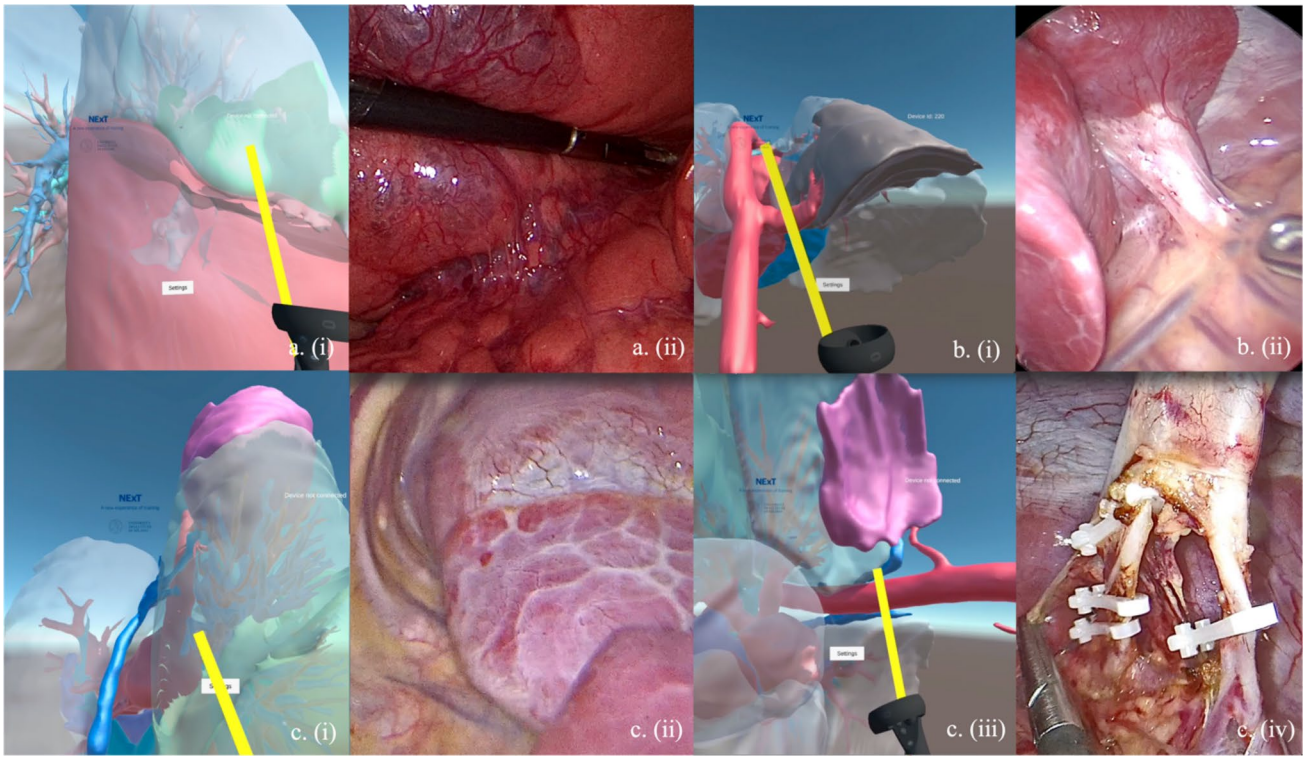


Fig. 2 Intraoperative correlation between thoracoscopic findings and immersive virtual reality (VR) reconstructions in different types of congenital pulmonary malformations (CPMs). For each condition, preoperative VR-based anatomical visualization is shown alongside the corresponding intraoperative thoracoscopic view, highlighting the anatomical concordance between virtual planning and surgical findings. **a** Congenital pulmonary airway malformation (CPAM) of the right middle lobe. (i) Immersive VR reconstruction illustrating the malformation and its segmental extension within the lobe, supporting spatial orientation and surgical planning. (ii) Corresponding thoracoscopic view confirming the cystic parenchymal involvement and its relationship with surrounding lung tissue. **b** Intralobar pulmonary sequestration. (i) Preoperative VR visualization clearly depicting the anomalous systemic feeding artery arising from the descending aorta (yellow marker). (ii) Intraoperative thoracoscopic identification and control of the systemic arterial supply during dissection. **c** Extralobar pulmonary sequestration. From left to right: (i) immersive VR overview showing the spatial relationship between the sequestrated mass and the adjacent lung parenchyma. (ii) Thoracoscopic view demonstrating the well-encapsulated appearance of the lesion. (iii) VR-based identification of the systemic arterial supply and venous drainage (yellow marker), aiding preoperative risk assessment and surgical strategy. (iv) Intraoperative confirmation and division of the vascular pedicle during thoracoscopic isolation of the lesion

alone. No multivariable or propensity-adjusted estimate was attempted because the limited sample size would have produced unstable estimates and would not have eliminated unmeasured era-related confounding. Additional analyses were performed according to four predefined malformation groups: CPAM, intralobar sequestration, extralobar sequestration, and other malformations. Focused sensitivity analyses evaluated CPAM plus intralobar sequestration and lobectomy-only cases; complete pathology-stratified comparisons and the remaining sensitivity analyses are provided in Supplementary Table S1. A chronological learning curve analysis was performed using case order and operative time, with VR introduction marked graphically. Statistical analyses were performed using Stata 19.0, and a two-sided $p < 0.05$ was considered statistically significant. No correction for multiple comparisons was applied.

Ethical approval

The study was performed in accordance with the ethical standards of the institutional and national research committees and with the 1964 Helsinki Declaration and its later amendments. The research protocol was approved by the Ethics Committee of the "Vittore Buzzi" Children's Hospital, Milano, Italy and registered in the Experimental Research Registry (No. 2022/ST/079, "RV and 3D models for simulation and research in pediatrics").

Results

Eighty-six consecutive infants underwent surgery for CPM during the study period. For this analysis, only those who underwent thoracoscopic resection were included, while patients treated by open surgery were excluded to avoid approach-related confounding. The final cohort comprised 50 thoracoscopic cases, divided according to the preoperative planning strategy: 39 (78%) planned with SI and 11 (22%) with the integrated patient-specific 3D segmentation and immersive VR navigation workflow (VR).

Population characteristics

Baseline demographic and perinatal characteristics were largely comparable between the two groups. The median gestational age at birth was 39.0 weeks (IQR: 38.0–40.0), and the mean birth weight was 3.1 ± 0.5 kg, with a mean length of 49.3 ± 2.7 cm and head circumference of 33.6 ± 1.6 cm. Most infants were male (29/50, 58%) and delivered vaginally (38/50, 76%), while cesarean delivery occurred in 10/50 (20%); these proportions were similar across both groups. Prenatal suspicion of CPM was documented in 45/50 (92%) cases, and prenatal symptoms were reported in 5/50 (10%), with no relevant intergroup differences. Histopathological diagnoses included CPAM in 18/50 (36%), extralobar pulmonary sequestration in 14/50 (28%), intralobar pulmonary sequestration in 11/50 (22%), bronchial atresia in 4/50 (8%), bronchogenic cyst in 2/50 (4%), and lobar overinflation in 1/50 (2%). Bronchogenic cysts were found only in the VR group (2/11, 18%), while extralobar sequestrations predominated among patients planned with standard imaging (13/39, 33%). Associated maternal gestational conditions were recorded in 10/50 (30%) of the overall population. Congenital cardiac or vascular anomalies were detected in 12/50 (24%), more frequently among VR-planned patients (5/11, 45%) than in those with standard planning (7/39, 18%). Other associated anomalies were less common, including urinary tract defects in 6/50 (12%), central nervous system (CNS) anomalies in 3/50 (6%), and gastrointestinal (GI) anomalies in 4/50 (8%), with similar distribution between groups. The malformation involved the left side in 31/50 (62%) and the right side in 19/50 (38%). Respiratory symptoms before surgery were reported in 9/37 (24%) SI patients and 2/11 (18%) VR patients ($p = 1.000$). Recurrent airway infection before surgery was reported in 7/37 (19%) SI patients and 2/11 (18%) VR patients ($p = 1.000$); data were unavailable for two SI patients. At the time of surgery, half of the patients were classified as ASA II (25/50, 50%), and 20/50 (40%) as ASA III. The median age at surgery was 8.5 months (IQR: 6.0–16.0), comparable between groups (Table 1).

Surgical characteristics

All procedures were performed thoracoscopically. Overall, 23/50 (46%) underwent lobectomy and 27/50 (54%) a lung-sparing resection. Lobectomy was more frequent among VR-planned cases (7/11, 64%) compared with those planned with standard imaging (16/39, 41%, p value = 0.18). The median anesthesia time for the entire cohort was 372.5 min (IQR 294.0–479.0), numerically shorter in the VR group (334.5 min [262.0–450.0]) than in the SI group (376.5 min [296.0–496.5], p value = 0.35). Similarly, the median operative time was 235.0 min (IQR 149.0–315.0) overall, lower in the VR group (183.0 min [127.0–302.0]) compared with standard imaging (248.0 min [150.0–315.0], p value = 0.42). Although these differences were not statistically significant, the numerical direction remained clinically noteworthy, particularly because lobectomy was more frequent in the VR group. Conversion to open surgery occurred in 10/50 (20%), all within the SI group (10/39, 26%) and none among VR-planned procedures (0/11, 0%). This difference reached statistical significance (p value = 0.045). Intraoperative complications were recorded in 5/50 (10%), all in the SI group (5/39, 13%) and none in the VR group (0/11, 0%, p value = 0.20) (Table 2). These findings represent unadjusted

Table 1 Baseline demographic and perinatal characteristics of the study population

Variable	Virtual reality ($n=11$)	Standard imaging ($n=39$)	Overall ($n=50$)	p value
Gestational age (weeks), median (IQR)	39.0 (38.0–40.0)	39.0 (38.0–40.0)	39.0 (38.0–40.0)	0.85
Birth weight (kilograms), mean ± SD	3.1 ± 0.5	3.1 ± 0.5	3.1 ± 0.5	0.94
Length (centimeters), mean ± SD	49.8 ± 1.7	49.2 ± 2.9	49.3 ± 2.7	0.66
Head circumference (centimeters), mean ± SD	33.1 ± 2.3	33.7 ± 1.3	33.6 ± 1.6	0.41
Male gender, *n* (%)	6 (55)	23 (59)	29 (58)	0.79
Vaginal delivery, *n* (%)	10 (91)	28 (72)	38 (76)	0.40
Cesarean section, *n* (%)	1 (9)	9 (23)	10 (20)	–
Prenatal diagnosis, *n* (%)	9 (90)	36 (92)	45 (92)	0.81
Maternal gestational disorder, *n* (%)	0 (0)	10 (40)	10 (30)	0.032
Lesion side, *n* (%)				
Left	5 (45)	26 (67)	31 (62)	0.20
Right	6 (55)	13 (33)	19 (38)	
Associated anomalies, *n* (%)	4 (36)	18 (47)	22 (45)	0.52
CVS defect	5 (45)	7 (18)	12 (24)	0.066
Urinary tract anomalies	0 (0)	6 (16)	6 (12)	0.16
CNS anomalies	1 (9)	2 (5)	3 (6)	0.64
GI anomalies	0 (0)	4 (11)	4 (8)	0.26
Respiratory symptoms before surgery, *n/N* (%)	2/11 (18)	9/37 (24)	11/48 (23)	1.000
Recurrent airway infection before surgery, *n/N* (%)	2/11 (18)	7/37 (19)	9/48 (19)	1.000

Denominators vary where clinical data were unavailable

IQR interquartile range, *SD* standard deviation, *CVS* cardiovascular, *CNS* central nervous system, *GI* gastrointestinal

Table 2 Operative characteristics of infants undergoing thoracoscopic surgery for congenital pulmonary malformations

Variable	Virtual reality ($n=11$)	Standard imaging ($n=39$)	Overall ($n=50$)	p value
Age at surgery (months), median (IQR)	8.0 (6.0–46.0)	9.0 (6.0–16.0)	8.5 (6.0–16.0)	0.92
ASA, *n* (%):				
II	6 (55)	19 (49)	25 (50)	0.94
III	4 (36)	16 (41)	20 (40)	
Type of surgery, *n* (%):				
Lobectomy	7 (64)	16 (41)	23 (46)	0.18
Lung-sparing resection	4 (36)	23 (59)	27 (54)	
Anesthesia time (minutes), median (IQR)	334.5 (262.0–450.0)	376.5 (296.0–496.5)	372.5 (294.0–479.0)	0.35
Operative time (minutes), median (IQR)	183.0 (127.0–302.0)	248.0 (150.0–315.0)	235.0 (149.0–315.0)	0.42
Conversion, *n* (%)	0 (0)	10 (26)	10 (20)	0.045
Intraoperative complications, *n* (%)	0 (0)	5 (13)	5 (10)	0.20
Blood transfusion, *n* (%)	5 (56)	23 (72)	28 (68)	0.35

IQR interquartile range

historical comparisons and should be interpreted together with the study limitations.

Postoperative outcomes and follow-up

Postoperative recovery showed favorable differences for patients whose procedures were planned with VR. The median time to extubation was 1.0 day (IQR: 0.0–1.0) in the SI group and 0.0 days (IQR: 0.0–0.0) in the VR group (p-value = 0.11). Nearly, all patients required postoperative intensive or intermediate care (46/50, 98%), with 36/39 (97%) in the SI group and 10/10 (100%) in the VR group (p value = 0.60). The median NICU/PICU length of stay was 2.0 days (IQR: 1.0–3.0) overall, reduced from 2.0 days (IQR:

1.0–3.0) in the SI group to 1.0 day (IQR: 1.0–2.0) in the VR group (p value = 0.045). The total length of hospital stay was 7.0 days (IQR: 5.0–9.0) for the whole cohort, significantly shorter in the VR group (5.0 days [4.0–6.0]) than in the SI group (8.0 days [6.0–10.0], p value < 0.001). Postoperative complications occurred in 6/50 (12%), all in the standard imaging group (6/39, 15%) and none in the VR group (0/11, 0%, p value = 0.16). According to the Clavien–Dindo classification, complications were grade II in 1/50 (2%), grade IIIb in 4/50 (8%), and grade IV in 1/50 (2%); no complications were reported in the VR group (p-value = 0.59). Blood transfusion was required in 28/50 (68%), with a lower incidence in the VR group (5/11, 56%) compared with the SI group (23/39, 72%, p value = 0.35). Redo surgery was necessary in 3/50 (6%), all following standard imaging planning (3/39, 8% SI vs 0/11, 0% VR; p-value = 0.34) (Table 3). The median duration of postoperative follow-up was 63.0 months (IQR: 31.0–109.5) for the overall cohort, significantly longer in the SI group (74.0 months [54.0–126.0]) compared with the VR group (24.5 months [9.0–32.0], p value < 0.001), reflecting the more recent introduction of VR planning. A graphical representation of the main perioperative and postoperative outcomes comparing the SI and VR groups is shown in Fig. 3.

Malformation-specific and chronological analyses

To address potential case-mix heterogeneity, patients were further stratified into four predefined malformation groups: CPAM, intralobar sequestration, extralobar sequestration, and other malformations. The overall clinical and surgical profile of these groups, pathology-stratified comparisons between SI and VR planning, and sensitivity analyses are summarized in Supplementary Table S1. Relevant heterogeneity was observed across malformation groups in operative time, hospital length of stay, lobectomy rate, conversion rate, and composite adverse outcome.

In pathology-stratified comparisons, the clearest favorable signal was observed among patients with CPAM, whereas findings in intralobar sequestration, extralobar sequestration, and other malformations were more limited and should be interpreted cautiously because of sparse data. Focused sensitivity analyses restricted to CPAM plus intralobar sequestration and to lobectomy-only cases showed that the favorable direction of hospital stay and composite adverse outcomes was maintained. Among patients with CPAM or intralobar sequestration, median hospital stay was 10.0 days (IQR 8.0–13.0) in the SI group and 5.0 days (4.8–6.0) in the VR group ($p < 0.001$), while the composite adverse outcome occurred in 13/19 SI patients and 0/8 VR patients ($p = 0.002$). In lobectomy-only cases, median hospital stay was 9.0 days (7.0–12.5) in the SI group and 5.0 days (5.0–6.0) in the VR group ($p < 0.001$), while the composite adverse outcome occurred in 8/15 SI patients and 0/7 VR patients ($p = 0.022$). These subgroup findings are preliminary because of the small, non-concurrent samples, but their consistent direction supports further targeted evaluation.

The chronological learning curve analysis is shown in Fig. 4. VR planning was introduced in the later phase of the study period, and VR-planned cases were therefore temporally clustered after the initial standard imaging experience. Operative times were widely dispersed in both groups and no consistent downward trend was observed after VR introduction; several later VR cases had longer operative times. Nevertheless, no intraoperative or postoperative complications were observed among VR-planned cases. The chronological distribution confirms the potential influence of institutional learning curve and era effects, which cannot be separated from a possible contribution of the VR workflow in this dataset.

Table 3 Postoperative outcomes and follow-up after thoracoscopic surgery for congenital pulmonary malformations

Variable	Virtual reality ($n = 11$)	Standard imaging ($n = 39$)	Overall ($n = 50$)	p value
Postoperative extubation (days), median (IQR)	0.0 (0.0–0.0)	1.0 (0.0–1.0)	1.0 (0.0–1.0)	0.11
Postoperative NICU/PICU admission, n (%)	10 (100)	36 (97)	46 (98)	0.60
NICU/PICU stay (days), median (IQR)	1.0 (1.0–2.0)	2.0 (1.0–3.0)	2.0 (1.0–3.0)	0.045
Hospital stay (days), median (IQR)	5.0 (4.0–6.0)	8.0 (6.0–10.0)	7.0 (5.0–9.0)	< 0.001
Postoperative complications, n (%)	0 (0)	6 (15)	6 (12)	0.16
Clavien–Dindo grade, n (%)				
II	0 (0)	1 (3)	1 (2)	0.59
III	0 (0)	4 (10)	4 (8)	
IV	0 (0)	1 (3)	1 (2)	
Redo surgery, n (%)	0 (0)	3 (8)	3 (6)	0.34
Follow-up (months), median (IQR)	24.5 (9.0–32.0)	74.0 (54.0–126.0)	63.0 (31.0–109.5)	< 0.001

IQR interquartile range, *NICU* neonatal intensive care unit, *PICU* pediatric intensive care unit

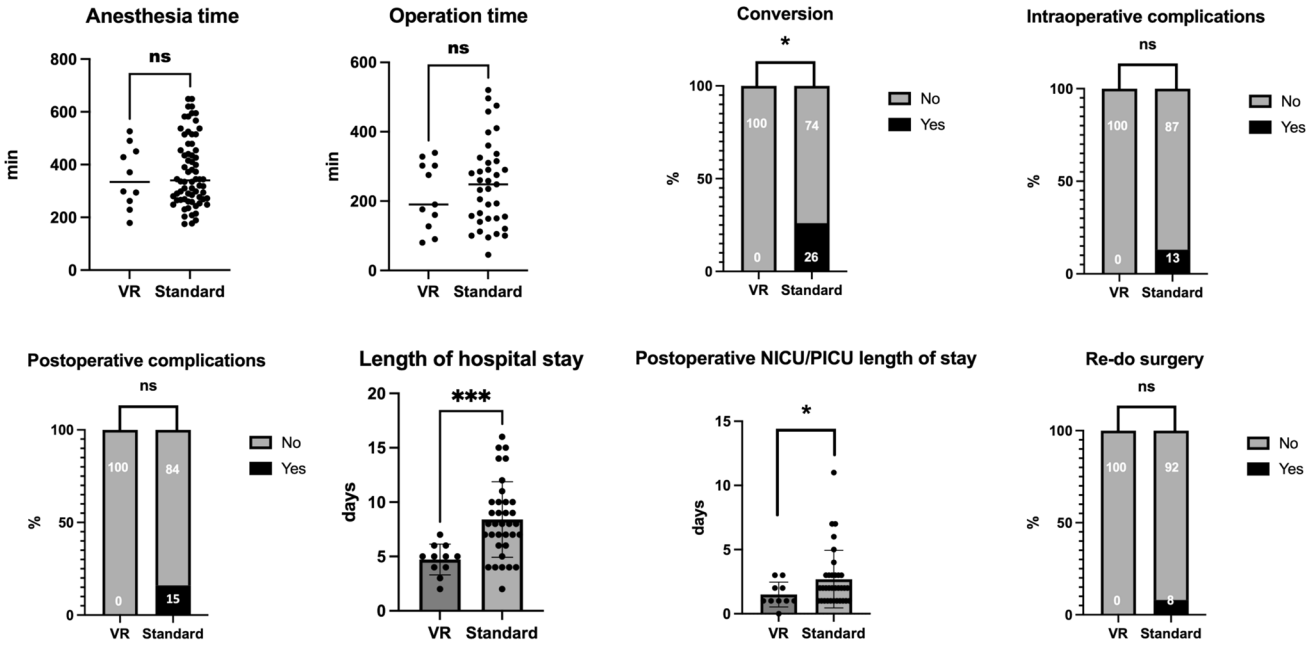


Fig. 3 Graphical representation of perioperative and postoperative outcomes comparing the standard imaging group and the virtual reality (VR) group for thoracoscopic resection of congenital pulmonary malformations

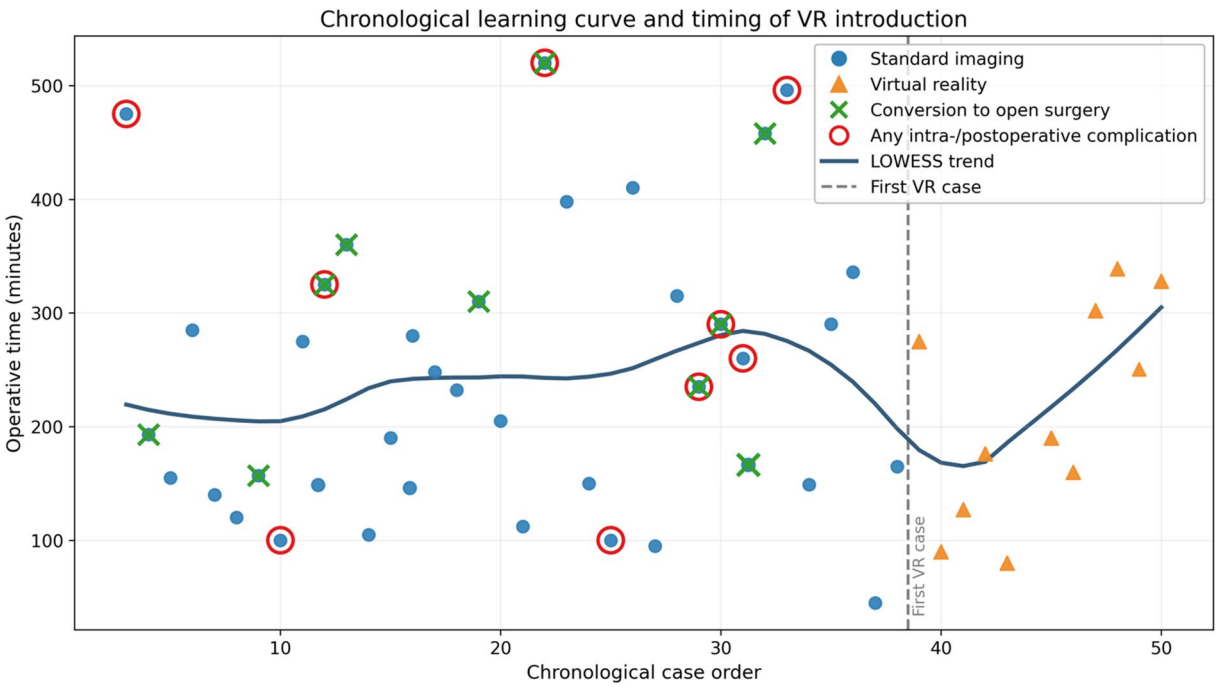


Fig. 4 Chronological learning curve and timing of VR introduction. Each point represents one thoracoscopic case ordered by surgery date. Blue circles indicate standard imaging and orange triangles VR planning. Green crosses indicate conversion to open surgery, while red outlined circles indicate intraoperative and/or postoperative complications. The blue-gray line shows the LOWESS-smoothed operative time trend, and the dashed vertical line marks the first VR-planned case. The trend is descriptive and should not be interpreted as evidence of a consistent reduction in operative time after VR introduction

Discussion

Thoracoscopic surgery has progressively become a preferred approach for the management of congenital pulmonary malformations, offering the advantages of minimally invasive surgery while preserving the need for precise anatomical dissection in a small operative field [6]. Nevertheless, this approach remains technically demanding because of limited intrathoracic working space, variable bronchovascular anatomy, and the need to preserve healthy lung parenchyma [8]. In this context, the integration of 3D segmentation and immersive VR navigation represents a promising advancement in preoperative planning and team preparation [8, 9]. In the present preliminary single-center historical cohort, VR-guided planning was feasible and was associated with favorable perioperative signals, including shorter hospital stay and no observed conversions or complications among VR-planned cases. The historical comparison does not establish causality; however, the concordant direction of several clinically relevant outcomes provides meaningful preliminary evidence and supports further evaluation of this novel planning strategy.

The demographic and perinatal profile of our 50-patient cohort was consistent with most current series. The male-to-female ratio (1.4:1), median gestational age of 39 weeks, and mean birth weight of 3.1 kg were comparable to the data reported by Zhao et al. [13] in a multicenter analysis of 173 patients. Similarly, more than 90% of our patients were diagnosed prenatally, consistent with the increasing detection rates seen in European and Asian registries [5, 13]. All patients underwent thoracoscopic resection, with a median age at surgery of 8.5 months. This timing is consistent with current recommendations that elective resection during infancy, typically between 6 and 12 months, optimizes postoperative recovery and compensatory lung growth while minimizing adhesion-related difficulties [13, 14]. In this regard, Pio et al. [15] demonstrated that lobectomy before 5 months of age preserves pulmonary function without increasing complications, while Zhao et al. [13] found that earlier surgery significantly reduced adhesions and conversion risk. Our results are therefore broadly consistent with contemporary thoracoscopic series.

The median operative time in our overall cohort was similar to previously published averages for thoracoscopic lobectomy in infants [13, 16–19]. The shorter duration observed in the VR group (183 min) compared with the SI group (248 min) did not reach statistical significance and should not be interpreted as proof that VR reduces operative time. However, this numerical difference occurred despite a higher proportion of lobectomies in the VR cohort, which preserves clinical interest in the observed signal. López-Díaz et al. [19] reported a median of 170 min, with a significant association between operative duration and increased complication rate ($p = 0.002$). In our data, the absence of complications in the VR group paralleled numerically shorter anesthesia and operative times, although the chronological analysis showed substantial variability and no consistent downward trend. Conversion to thoracotomy remains one of the main quality indicators in minimally invasive thoracic surgery.

Conversion rates in the literature vary from 2 to 30%, depending on patient age, surgeon experience, lesion type and previous infection [7, 14, 15, 18, 19]. In our study, no conversions occurred in the VR group (0%) compared with 26% in the SI group, a difference that reached statistical significance (p value = 0.045). The non-concurrent design prevents attribution of this difference specifically to VR; nevertheless, the absence of conversion in the 11 VR-planned cases remains a clinically relevant preliminary signal, particularly because the VR cohort included a higher proportion of lobectomies and more frequent cardiac or vascular anomalies. Patient-specific navigation may plausibly support anticipation of anomalous vessels and bronchial anatomy, a hypothesis that warrants prospective testing.

The overall complication rate in our cohort (12%) was entirely attributable to events in the SI group, and it falls within the broad range reported in large thoracoscopic series, where postoperative morbidity after thoracoscopic lobectomy for CPM generally varies between 10 and 30% [7, 13, 14, 16, 20]. By contrast, no intra- or postoperative complications were observed among VR-planned procedures. Although the differences did not reach statistical significance because of the small number of events, this complication-free experience is consistent with the proposed role of immersive planning in supporting safer dissection and controlled vascular management. It should be considered a favorable safety signal rather than proof of superiority.

Postoperative recovery indicators favored VR-guided planning. The median NICU/PICU stay was reduced from two to one day ($p = 0.045$), and total hospital stay decreased from eight to five days (p value < 0.001). In comparison, Mattioli et al. [21] found a median hospital stay of 4 days after thoracoscopy versus nine days after thoracotomy (p value = 0.0009); López-Díaz et al. [19] reported 5 days after the learning curve plateau; and Zhao et al. [13] documented seven days across all ages. Thus, the shorter hospital stay observed in the VR group represents a clinically relevant preliminary signal. Changes in postoperative management and discharge practice over time may have contributed to this difference, but the magnitude and consistency of the observation justify prospective assessment rather than dismissal of a possible workflow-related benefit.

Early extubation was achieved in all VR cases (median 0 days vs 1 day, p value = 0.11), consistent with reports of

rapid postoperative recovery after elective thoracoscopy in asymptomatic infants [14]. If confirmed in contemporaneous cohorts, these differences could translate into meaningful benefits for patients and healthcare systems, including reduced intensive-care use and hospital stay.

Only 3 patients (8%) in the SI group required redo surgery, a rate consistent with those reported in other pediatric thoracoscopic series (range 5–10%) [16, 18, 19]. However, in contrast with most literature reports, where redo procedures are typically related to postoperative air leaks or bronchopleural fistulae, the secondary interventions in our cohort were performed for residual disease and persistent localized infection, rather than for technical complications of the primary procedure. No reoperations were necessary in the VR group. This observation supports the hypothesis that detailed patient-specific planning may assist assessment of lesion boundaries, although the shorter follow-up of the VR cohort precludes conclusions regarding long-term recurrence.

The improvement seen between our earlier standard imaging (SI) and later virtual reality (VR)-assisted cases parallels the learning curve effects described by López-Díaz et al. [19] and Seong et al. [16], who found that conversion and complication rates decreased with increasing experience. This temporal relationship is an important confounder, but it does not exclude a complementary contribution from immersive planning.

Our VR series achieved favorable outcomes during a mature phase of the institutional program. By virtually navigating the hilar structures and defining trocar trajectories in advance, the workflow may have supported operative preparation, team coordination, and reduction of cognitive load. The present study cannot quantify the independent contribution of these mechanisms, but the observations are compatible with the intended function of the technology.

Importantly, the potential learning curve effect in this study should not be interpreted as a simple transition from inexperienced to experienced surgeons, as all procedures were performed or directly supervised by pediatric surgeons with established expertise in thoracoscopic surgery. Rather, it likely reflects maturation of an institutional pathway over time, including greater team familiarity, refinement of thoracoscopic technique, improved perioperative management and increasing experience with patient-specific 3D/VR planning. Accordingly, the observed outcomes probably reflect the combined influence of institutional maturation and the new planning workflow; the relative contribution of each cannot be separated in this retrospective dataset.

VR planning adds an interactive dimension to preoperative assessment. The conventional cross-sectional imaging contains the same underlying anatomical information and that experienced surgeons and radiologists can mentally reconstruct three-dimensional relationships. However, mental reconstruction is not equivalent to direct stereoscopic navigation of a shared patient-specific model. Immersive VR allows the surgeon to enter and interact with the patient's anatomy, explore the broncho-vascular tree from multiple perspectives, adjust transparency, reproduce the thoracoscopic orientation and share the same view with the multidisciplinary team. This concept was previously evaluated by Pelizzo et al. [8, 9] using head-mounted displays in congenital and oncologic cases, where VR planning altered surgical strategy and improved trainees' spatial orientation and operative confidence. The novelty of our approach therefore lies not in generating new anatomical information, but in transforming that information into an interactive and navigable planning environment. The present study evaluates the integrated workflow as a whole and cannot isolate the contribution of segmentation, rendering or the headset.

In our workflow, the VR session became an integral component of the multidisciplinary preoperative planning process. The patient-specific 3D model, oriented to replicate the intraoperative lateral decubitus position, facilitated trocar mapping and discussion of the sequence of vessel division. Moreover, surgeons, radiologists, anesthesiologists and trainees could visualize the same immersive scene, enabling shared mental modeling of potential challenges, a feature previously associated with improved team communication [22]. These cognitive and team benefits may have contributed to the favorable perioperative signals observed, although they were not directly measured.

Beyond clinical planning, immersive VR also offers an educational environment in which trainees and young surgeons can repeatedly review broncho-vascular relationships, uncommon anatomical variations and the anticipated sequence of dissection before surgery. Surgeon confidence, anatomical understanding, cognitive workload, and educational performance were not formally assessed in the present study and should be evaluated using validated instruments in future prospective work.

The additional malformation-specific analyses directly address the concern that different congenital pulmonary malformations entail different operative complexity. CPAM and intralobar sequestration represented the subgroups in which the potential value of VR planning appeared most clinically relevant, likely because these lesions often require careful interpretation of lobar anatomy, vascular supply, and resection planes. By contrast, extralobar sequestration generally had shorter operative time and hospital stay, and its resection is not directly comparable with lobectomy. The favorable direction of the findings was maintained in the focused CPAM-plus-intralobar sequestration and lobectomy-only analyses. Although these small subgroups remain hypothesis generating, their consistency strengthens the rationale for evaluating VR prospectively in anatomically complex lesions rather than assuming a uniform effect across all

malformations. Similarly, Destro et al. demonstrated that VR combined with echo-endoscopy offers a whole perspective of hepatobiliary anatomy, facilitating safer minimally invasive interventions [23].

Limitations

This study should be interpreted in light of its retrospective single-center design and the small size of the VR cohort, which limit statistical power and causal inference. Because VR planning was introduced later in the institutional experience, the observed outcome differences may partly reflect era effects, maturation of the thoracoscopic program, refinements in surgical technique, team coordination, anesthesia, analgesia, postoperative pathways and discharge practices. Although chronological and focused pathology- and procedure-based analyses were performed, they cannot fully separate the contribution of VR from broader institutional experience, and subgroup analyses remain limited by small numbers. Residual differences in previous respiratory infection, inflammatory adhesions, anatomical complexity and case selection may also have influenced the outcomes. The intervention comprised an integrated workflow combining patient-specific segmentation, 3D reconstruction and immersive navigation; consequently, the contribution of each individual component cannot be isolated. The workflow requires high-quality imaging, segmentation expertise, dedicated software and multidisciplinary review, which may affect generalizability to lower-volume centers. Finally, the absence of conversion or complications in 11 VR-planned patients and the shorter postoperative recovery should be interpreted as preliminary signals rather than proof of superiority. These limitations temper, but do not negate, the clinical relevance of the consistent associations observed and the need for prospective validation.

Future perspectives

Prospective, multicenter studies with contemporaneous comparison groups and clinically homogeneous procedures are needed to determine whether the favorable signals observed here persist after accounting for lesion type, previous infection, surgeon and institutional experience, and standardized perioperative pathways. Studies comparing conventional cross-sectional imaging, desktop patient-specific 3D visualization and immersive navigation could help distinguish the contribution of individual workflow components. The integration of automated segmentation, augmented reality overlays, and intraoperative fluorescence imaging could link preoperative VR models directly to the surgical field [24, 25]. Standardized training curricula incorporating VR simulation may shorten the learning curve for pediatric surgeons, similar to its established role in adult laparoscopic and robotic education [26–28]. Future studies should also assess anatomical understanding, operative preparedness, surgeon confidence, cognitive workload, and knowledge retention using validated measures. Beyond planning, VR could serve as a communication tool for families, enhancing informed consent through intuitive visualization of the malformation and surgical plan.

Conclusion

In this preliminary single-center historical cohort, the integrated patient-specific 3D segmentation and immersive VR navigation workflow was feasible and was associated with favorable perioperative signals after thoracoscopic resection of congenital pulmonary malformations, including shorter hospital stay and lower observed rates of conversion and complications. The favorable direction was maintained in focused analyses of more comparable lesions and procedures, supporting VR as a promising adjunct to patient-specific preoperative preparation. Because of the small VR cohort, chronological separation between groups and lesion and procedure heterogeneity, these results do not prove superiority or an independent causal effect. Nevertheless, they provide clinically relevant preliminary evidence and justify prospective multicenter studies designed to determine which patients and procedures may benefit most from immersive planning.

Supplementary Information The online version contains supplementary material available at https://doi.org/10.1007/s00464-026-13307-1.

Author contributions All listed authors contributed substantially to this manuscript and approved the final submitted version. The specific contributions are as follows: conceptualization: UMP and GP; methodology, validation, and resources: UMP, IP, SC; FR, CG, MV, and GP; investigation: UMP, IP, AM, CA, MM, MC, ED, SB, SZ, FR, and CG; data curation, writing—original draft preparation, visualization, and project administration: UMP and IP; writing—review and editing: UMP, IP, FR, CG, MV, GZ, and GP; supervision: VC, GZ, and GP.

Funding This work was supported within the Multilayered Urban Sustainability Action (MUSA)—project, funded by the European Union—NextGenerationEU, under the National Recovery and Resilience Plan (NRRP) Mission 4 Component 2 Investment Line 1.5: Strengthening of research structures and creation of R&D "innovation ecosystems," set up of "territorial leaders in R&D." We gratefully acknowledge the Foundation Romeo and Enrica Invernizzi and Leonardo LoCascio Foundation for supporting this project.

Data availability The data supporting the findings of this study are available from the corresponding author upon reasonable request, subject to institutional and ethical requirements. No publicly archived dataset was generated for this retrospective study.

Declarations

Disclosures Ugo Maria Pierucci, Irene Paraboschi, Sara Costanzo, Carlotta Ardenghi, Michela Marinaro, Alessia Musitelli, Michele

Ceresola, Eleonora Durante, Sara Baroni, Francesco Rizzetto, Salvatore Zirpoli, Cristina Gallotta, Maurizio Vertemati, Valeria Calcaterra, Gianvincenzo Zuccotti, and Gloria Pelizzo have no conflicts of interest or financial ties to disclose.

References

1. Pederiva F, Rothenberg SS, Hall N, Ijsselstijn H, Wong KKY, Von Der Thüsen J, Ciet P, Achiron R, Pio d'Adamo A, Schnater JM (2023) Congenital lung malformations. Nat Rev Dis Primers 9:60. https://doi.org/10.1038/s41572-023-00470-1
2. Wong KKY, Flake AW, Tibboel D, Rottier RJ, Tam PKH (2018) Congenital pulmonary airway malformation: advances and controversies. Lancet Child Adolesc Health 2:290–297. https://doi.org/10.1016/S2352-4642(18)30035-X
3. Nadeem M, Elnazir B, Greally P (2012) Congenital pulmonary malformation in children. Scientifica 2012:1–7. https://doi.org/10.6064/2012/209896
4. Rothenberg SS (2003) Experience with thoracoscopic lobectomy in infants and children. J Pediatr Surg 38:102–104. https://doi.org/10.1053/jpsu.2003.50020
5. Morini F, Zani A, Conforti A, Van Heurn E, Eaton S, Puri P, Rintala R, Lukac M, Kuebler J, Friedmacher F, Wijnen R, Tovar J, Pierro A, Bagolan P (2018) Current management of congenital pulmonary airway malformations: a "European Pediatric Surgeons' Association" survey. Eur J Pediatr Surg 28:001–005. https://doi.org/10.1055/s-0037-1604020
6. Rothenberg SS (2021) Thoracoscopic lobectomy in infants and children. J Laparoendosc Adv Surg Tech A 31:1157–1161. https://doi.org/10.1089/lap.2021.0454
7. Rothenberg SS, Middlesworth W, Kadennhe-Chiweshe A, Aspelund G, Kuenzler K, Cowles R, Bodenstein L, Kay S, Shipman K, Rothenberg C, Stolar C, Stylianos S (2015) Two decades of experience with thoracoscopic lobectomy in infants and children: standardizing techniques for advanced thoracoscopic surgery. J Laparoendosc Adv Surg Tech A 25:423–428. https://doi.org/10.1089/lap.2014.0350
8. Pelizzo G, Costanzo S, Roveri M, Lanfranchi G, Vertemati M, Milani P, Zuccotti G, Cassin S, Panfili S, Rizzetto F, Campari A, Camporesi A, Calcaterra V (2022) Developing virtual reality head mounted display (HMD) set-up for thoracoscopic surgery of complex congenital lung malformations in children. Children (Basel) 9:50. https://doi.org/10.3390/children9010050
9. Pelizzo G, Pierucci UM, Marinaro M, Costanzo S, Durante E, Ardenghi C, Musitelli A, Milani P, Rizzetto F, Vertemati M, Campari A, Barisella M, Santaniello T, Gallotta C, Camporesi A, Paraboschi I, Varrica A, Alberti D, Calcaterra V, Zuccotti G (2025) Virtual reality for preoperative planning and education in pediatric surgery: preliminary results for the treatment of congenital malformations and tumors. World J Surg 49:1497–1507. https://doi.org/10.1002/wjs.12594
10. Fedorov A, Beichel R, Kalpathy-Cramer J, Finet J, Fillion-Robin J-C, Pujol S, Bauer C, Jennings D, Fennessy F, Sonka M, Buatti J, Aylward S, Miller JV, Pieper S, Kikinis R (2012) 3D Slicer as an image computing platform for the Quantitative Imaging Network. Magn Reson Imaging 30:1323–1341. https://doi.org/10.1016/j.mri.2012.05.001
11. Wasserthal J, Breit H-C, Meyer MT, Pradella M, Hinck D, Sauter AW, Heye T, Boll DT, Cyriac J, Yang S, Bach M, Segeroth M (2023) TotalSegmentator: robust segmentation of 104 anatomic structures in CT images. Radiol Artif Intell 5:e230024. https://doi.org/10.1148/ryai.230024
12. Vertemati M, Cassin S, Rizzetto F, Vanzulli A, Elli M, Sampogna G, Gallieni M (2019) A virtual reality environment to visualize three-dimensional patient-specific models by a mobile head-mounted display. Surg Innov 26:359–370. https://doi.org/10.1177/1553350618822860
13. Zhao Y, Liu D, Wang Y, Niu Z, Jia H, Bai Y (2025) Elective thoracoscopic surgery for congenital lung malformations: what age to operate? Eur J Pediatr 184:165. https://doi.org/10.1007/s00431-025-05990-4
14. Elhattab A, Elsaied A, Wafa T, Jugie M, Delacourt C, Sarnacki S, Aly K, Khen-dunlop N (2021) Thoracoscopic surgery for congenital lung malformations: does previous infection really matter? J Pediatr Surg 56:1982–1987. https://doi.org/10.1016/j.jpedsurg.2021.01.036
15. Pio L, Jafar Y, Carvalho L, Ali L, Delcaux C, Julien-Marsollier F, Bonnard A (2025) Thoracoscopic lobectomy for congenital pulmonary airway malformations before or after 5 months of age: evaluation of pulmonary function. Minerva Pediatr. https://doi.org/10.23736/S2724-5276.23.07124-0
16. Seong YW, Kang CH, Kim J-T, Moon HJ, Park IK, Kim YT (2013) Video-assisted thoracoscopic lobectomy in children: safety, efficacy, and risk factors for conversion to thoracotomy. Ann Thorac Surg 95:1236–1242. https://doi.org/10.1016/j.athoracsur.2013.01.013
17. Tarrado X, Castañón M, Olivares M, García-Núñez B, Vancells M, Muñoz E, Ribó JM (2010) Thoracoscopic lobectomy: initial experience. Cir Pediatr 23:111–114
18. Esposito C, Bonnard A, Till H, Leva E, Khen-Dunlop N, Zanini A, Montalva L, Sarnacki S, Escolino M (2021) Thoracoscopic management of pediatric patients with congenital lung malformations: results of a European multicenter survey. J Laparoendosc Adv Surg Tech A 31:355–362. https://doi.org/10.1089/lap.2020.0596
19. López-Diaz M, Cano Novillo I, Morante-Valverde R, García Vázquez A, Romero Layos M, Galindo Izquierdo A, Antón-Pacheco JL (2025) Thoracoscopic lobectomy for congenital lung malformation in children: evolving management strategies and their impact in outcomes. J Pediatr Surg 60:161992. https://doi.org/10.1016/j.jpedsurg.2024.161992
20. Weller JH, Peter SDS, Fallat ME, Saito JM, Burns CR, Deans KJ, Fraser JD, Gadepalli SK, Helmrath MA, Hirschl RB, Kabre R, Lal DR, Landman MP, Leys CM, Mak GZ, Minneci PC, Wright TN, Kunisaki SM (2021) Thoracoscopic versus open lobectomy in infants with congenital lung malformations: a multi-institutional propensity score analysis. J Pediatr Surg 56:2148–2156. https://doi.org/10.1016/j.jpedsurg.2021.04.013
21. Mattioli G, Pio L, Disma NM, Torre M, Sacco O, Pistorio A, Zanaboni C, Montobbio G, Barra F, Ramenghi LA (2016) Congenital lung malformations: shifting from open to thoracoscopic surgery. Pediatr Neonatol 57:463–466. https://doi.org/10.1016/j.pedneo.2015.10.009
22. Robertson DJ, Abramson ZR, Davidoff AM, Bramlet MT (2024) Virtual reality applications in pediatric surgery. Semin Pediatr Surg 33:151387. https://doi.org/10.1016/j.sempedsurg.2024.151387
23. Destro F, Salerno R, Calcaterra V, Ardizzone S, Meroni M, Roveri M, Pierucci UM, Zaja A, Rizzetto F, Campari A, Vertemati M, Milani P, Pelizzo G (2023) Echo-endoscopy combined with virtual reality: a whole perspective of laparoscopic common bile duct exploration in children. Children (Basel) 10:760. https://doi.org/10.3390/children10040760
24. Wang X, Yang J, Zhou B, Tang L, Liang Y (2025) Integrating mixed reality, augmented reality, and artificial intelligence in complex liver surgeries: enhancing precision, safety, and outcomes. iLIVER 4:100167. https://doi.org/10.1016/j.iliver.2025.100167

25. Doornbos M-CJ, Peek JJ, Maat APWM, Ruurda JP, De Backer P, Cornelissen BMW, Mahtab EAF, Sadeghi AH, Kluin J (2024) Augmented reality implementation in minimally invasive surgery for future application in pulmonary surgery: a systematic review. Surg Innov 31:646–658. https://doi.org/10.1177/15533506241290412
26. Emmerling M, Tan H-J, Shirk J, Bjurlin MA (2023) Applications of 3-dimensional virtual reality models (Ceevra®) for surgical planning of robotic surgery. Urol Video J 18:100220. https://doi.org/10.1016/j.urolvj.2023.100220
27. Sardari Nia P, Olsthoorn JR, Heuts S, Maessen JG (2019) Interactive 3D reconstruction of pulmonary anatomy for preoperative planning, virtual simulation, and intraoperative guiding in video-assisted thoracoscopic lung surgery. Innov Technol Tech Cardiothorac Vasc Surg 14:17–26. https://doi.org/10.1177/1556984519826321
28. Oizumi H, Kanauchi N, Kato H, Endoh M, Suzuki J, Fukaya K, Sadahiro M (2011) Anatomic thoracoscopic pulmonary segmentectomy under 3-dimensional multidetector computed tomography simulation: a report of 52 consecutive cases. J Thorac Cardiovasc Surg 141:678–682. https://doi.org/10.1016/j.jtcvs.2010.08.027

Publisher's Note Springer Nature remains neutral with regard to jurisdictional claims in published maps and institutional affiliations.

Springer Nature or its licensor (e.g. a society or other partner) holds exclusive rights to this article under a publishing agreement with the author(s) or other rightsholder(s); author self-archiving of the accepted manuscript version of this article is solely governed by the terms of such publishing agreement and applicable law.